



Research article

PKC signal amplification suppresses non-small cell lung cancer growth by promoting p21 expression and phosphorylation

Shuyan Liu^{a,b,1}, Yayun Zhang^{b,1}, Qianyi Yang^b, Yingqiu Zhang^b, Han Liu^b, Mu-Hua Huang^{c,**}, Ruoyu Wang^{a,***}, Faqiang Lu^{a,*}^a Affiliated Zhongshan Hospital of Dalian University, Dalian, China^b Institute of Cancer Stem Cell, Dalian Medical University, Dalian, China^c School of Materials Science and Engineering, Beijing Institute of Technology, Beijing, China

ARTICLE INFO

Keywords:

PKC
Bisindolylmaleimide derivative
BD-15
p21
Phosphorylation
NSCLC

ABSTRACT

Protein kinase C (PKC) activation was previously associated with oncogenic features. However, small molecule inhibitors targeting PKC have so far proved ineffective in a number of clinical trials for cancer treatment. Recent progresses have revealed that most PKC mutations detected in diverse cancers actually lead to loss-of-function, thus suggesting the tumor-suppressive roles of PKC proteins. Unfortunately, the development of chemicals to enhance PKC activity is lagging behind relative to its small molecular inhibitors. Here, we report that a bisindolylmaleimide derivative (3,4-bis(1-(prop-2-ynyl)-1H-indol-3-yl)-1 H-pyrrole-2,5-dione, BD-15) significantly inhibited cell growth in non-small cell lung cancer (NSCLC). Mechanistically, BD-15 treatment resulted in markedly enhanced phosphorylation of PKC substrates and led to cell cycle arrest in G2/M. Further, BD-15 treatment upregulated p21 protein levels and enhanced p21 phosphorylation. BD-15 also promoted caspase3 cleavage and triggered cellular apoptosis. In xenograft mouse models, BD-15 exerted anti-tumor effects to suppress *in vivo* tumor formation. Collectively, our findings revealed the tumor-suppressive roles of BD-15 through enhancing PKC signaling and thus leading to upregulation of p21 expression and phosphorylation.

1. Introduction

Protein kinase C (PKC) family contains a group of Ser/Thr protein kinases that are implicated in diverse cellular functions including gene expression, cell proliferation, metastasis and differentiation. There are ten members in the PKC family that are further classified into three subfamilies: conventional PKC isozymes (α , β I, β II and γ), novel PKC isozymes (δ , ϵ , η and θ) and atypical PKC isozymes (ζ and ι) [1]. PKC was identified as the target for the tumor-promoting phorbol ester, and hence PKC was previously deemed as an oncoprotein that promotes tumorigenesis leading to the development of a number of PKC inhibitors as potential therapies. However, over 30 years of clinical research with PKC inhibitors has led to disappointing results, with even worse outcomes in some instances treated with PKC inhibitors [2, 3, 4]. Recently, Newton and colleagues have reported that loss-of-function PKC mutations occurred in diverse cancers, including colorectal cancer, head and neck

cancer, lung cancer, ovarian cancer, breast cancer, pancreatic cancer and hepatoma [5]. Another meta-analysis study of advanced **non-small cell lung cancer** (NSCLC) patients revealed that PKC inhibitors combined with chemotherapy led to decreased response rates and disease control rates compared with chemotherapy alone [6]. In addition, prolonged phorbol ester treatment was shown to reduce the levels of cPKC and nPKC isoforms [7]. These recent evidence challenges the established dogma and suggests that PKC actually acts as a tumor suppressor rather than an oncoprotein.

Emerging evidence has revealed the effectiveness of PKC activation in cancer inhibition through small molecules. The small molecule Roy-Bz is reported as the first PKC δ -selective activator in 2018. Roy-Bz inhibited colon cancer cell proliferation and migration in a PKC δ -dependent manner [8]. PKC activator 10-Me-aplog-1 also inhibited cancer cell growth that was dependent on PKC α in A549, as well as PKC α and PKC δ in SW260 and Colo-205(9). However, investigation on PKC activation

* Corresponding author.

** Corresponding author.

*** Corresponding author.

E-mail addresses: mhhuang@bit.edu.cn (M.-H. Huang), wangruoyu1963@163.com (R. Wang), faqiang3@163.com (F. Lu).¹ These authors contributed equally.

and the corresponding underlying mechanism have so far remained very limited. p21 is a key regulator in tumor progression, which effectively induces cell cycle arrest in G1/S and G2/M transitions. Nevertheless, p21 also functions in the inhibition of apoptosis [10, 11]. The phosphorylation of p21 is also involved in cancer development. Decreased expression of phosphorylated p21 was detected in gastric cancer tissues, particularly in patients with late-stage [12]. p21 phosphorylation was elevated in Fanbaicao and ursolic acid-induced apoptosis in human hepatoma cell HepG2 and colon adenocarcinoma cell SW480 [13, 14]. However, the potential effects of PKC signaling on p21 phosphorylation during cancer progression are still unclear.

Considering that PKC mutations are highly enriched in lung cancer, we evaluated the effects of a panel of bisindolylmaleimide derivatives on the non-small cell lung cancer A549 and H1299 cells, and identified 3,4-bis(1-(prop-2-ynyl)-1H-indol-3-yl)-1H-pyrrole-2,5-dione (BD-15) as a potent chemical to enhance PKC signaling. Our results revealed that BD-15 treatment significantly elevated the phosphorylation of PKC substrates and promoted p21 expression and phosphorylation, leading to cell cycle arrest and apoptosis.

2. Materials and methods

2.1. Synthesis of the compound BD-15

The compound 3,4-bis(1-(prop-2-ynyl)-1H-indol-3-yl)-1H-pyrrole-2,5-dione (BD-15) was synthesized according to the procedure reported [15], starting from indole 1 in 3 steps and 55% overall yield. The key step involved was the selective N-propargylation of arcyriarubin A. To a suspension of NaH (60% in oil, 192 mg, 4.80 mmol) in THF (8 mL) was added a solution of 4 (400 mg, 1.20 mmol) in THF (4 mL) at 0 °C under nitrogen atmosphere. The resulting mixture was stirred for 30 min and then treated with 1-bromopropyne (0.50 mL, 6.0 mmol) slowly. After the reaction mixture was stirred at 25 °C for 48 h, the reaction was quenched with sat. NH₄Cl (10 mL) at 0 °C, extracted with EtOAc. The combined organics were washed with water and brine in succession, then dried over anhydrous Na₂SO₄ and concentrated under vacuum. The residue was purified by flash column chromatography (FCC) with V (EtOAc)/V (Petroleum Ether) = 1/4 to afford the title compound as a red solid (401 mg, yield 83%). R_f = 0.54 [V (EtOAc)/V (Petroleum Ether) = 1/1]; m. p. 197 °C; IR (KBr, cm⁻¹): 3288 (m), 3048 (w), 2924 (w), 2121 (w), 1759 (m), 1698 (s), 1531 (s), 1465 (m), 1385 (m), 1335 (m), 1193 (m), 1177 (m), 739 (s); ¹H NMR (400 MHz, CDCl₃) δ (ppm): 7.80 (s, 2H), 7.41 (s, 1H), 7.37 (d, *J* = 8.0 Hz, 2H), 7.13 (t, *J* = 8.0 Hz, 2H), 6.95 (d, *J* = 8.0 Hz, 2H), 6.78 (t, *J* = 8.0 Hz, 2H), 4.91 (s, 4H), 2.44 (t, *J* = 4.0 Hz, 2H); ¹³C NMR (100 MHz, DMSO) δ(ppm): 173.2, 136.9, 132.0, 127.8, 126.6, 122.4, 121.6, 120.4, 110.8, 105.9, 79.1, 76.5, 35.9; HR-MS (EI): m/z 403.1327 [M]⁺ (C₂₆H₁₇N₃O₂⁺, required 403.1321).

2.2. Antibodies

Antibodies to PKCα, PKCβ, PKCγ, PKCε, and phospho-PKCα (Thr638) were purchased from Proteintech Group. Antibodies to p-PKC substrate and p-ERK were purchased from Cell Signaling Technology. Antibodies to p21 and GAPDH were obtained from Proteintech Group. Ki-67 antibody is from Sigma. Second infrared-labeled goat anti-rabbit and anti-mouse antibodies were obtained from LICOR. Secondary antibody rabbit anti-mouse IgG Alexa Fluorescence-488 for immunofluorescence is purchased from Invitrogen.

2.3. Cell culture

NSCLC cell lines A549 and H1299 cells were grown in RPMI-1640 medium with 10% fetal bovine serum (ExCell Bio, China) and 1% penicillin/streptomycin (Thermo-Fisher Scientific, USA). The cell lines were cultured at 37 °C in a humidified incubator with 5% CO₂.

2.4. Cell viability and proliferation assay

Cell viability was measured by MTT assay. In brief, A549 and H1299 cells were seeded in 96-well plate and followed by compound treatment for 24 h. Then, 20 μl per well MTT was added and the cells continued to be maintained in incubator for 4 h. After removing the media, 150 μl per well DMSO was added to dissolve formazan that is produced from MTT. Following 10 min with shaking, absorbance was recorded at OD570 with spectrometer.

Cell proliferation was detected with Ki-67 staining. After the treatment, cells were fixed with 4% paraformaldehyde (w/v) for 20 min, then permeabilized with 0.2% Triton-X100 for 5 min and blocked with goat serum for 30 min. After incubation with Ki-67 antibody for 30 min, cells were stained with second antibody for 30 min. DAPI was used to stain the nucleus. Ki-67 staining was observed with the fluorescent microscope (Leica, Germany).

2.5. Cell cycle

Cell cycle was monitored by flow cytometry [16]. Treated cells were collected and fixed with precooled 70% ethanol for 12 h at 4 °C. Then, cells were washed with PBS gently and incubated with propidium iodide (PI) at 20 μg/ml for 15 min at 37 °C, with 0.1% Triton-X100 and 100 μg/ml RNase A added. After that, cells were analyzed by ACCURI C6 flow cytometer (BD Bioscience, USA) and the data were analyzed with FlowJo software version 7.6.

2.6. Cell morphology

Morphologic changes of A549 and H1299 cells treated with the compound were detected with inverted phase-contrast microscopy.

2.7. Hoechst 33342 staining

A549 and H1299 cells were stained with Hoechst 33342 at 5 μg/ml in the medium for 10 min at 37 °C. After washed with PBS for two times, cells were observed under a fluorescence microscope. Apoptotic cells show intense local staining, while normal cells exhibit diffuse DNA staining.

2.8. Western blotting

Western blotting was conducted as described previously [17]. After treatment, cells were lysed and protein concentration was measured using the BCA protein assay kit (Thermo). Equal amounts of samples were applied to 8% SDS-PAGE gels and electroblotted onto nitrocellulose membranes (Merck Millipore). Following blocked with 4% non-fat milk for 1 h at room temperature, the membranes were incubated with primary antibodies overnight at 4 °C. Subsequently, after washing with PBST for three times, the membranes were probed with secondary antibodies for 1 h at room temperature. Finally, protein signals were detected by a LICOR Odyssey Imager. Protein levels were analyzed with Image Studio software.

2.9. In vivo anti-tumor assay

Animal experiments were conducted according to the National Institutes of Health Guide for the Care and Use of Laboratory Animals, and the approval was obtained for the protocol from the Institutional Animal Care and Use Committee at Dalian Medical University. Female BALB/c nude mice (–6-Week-old) were purchased from Vital River Laboratories in Beijing. 1 × 10⁶ A549 and 1 × 10⁶ H1299 cells were subcutaneously implanted in the dorsal flank of mice. After one week, mice implanted with A549 and H1299 cells were separately divided into two groups, with 5 mice carrying xenograft tumors with similar size in each. Mice in control group were injected with DMSO (in PBS). Another is BD-15

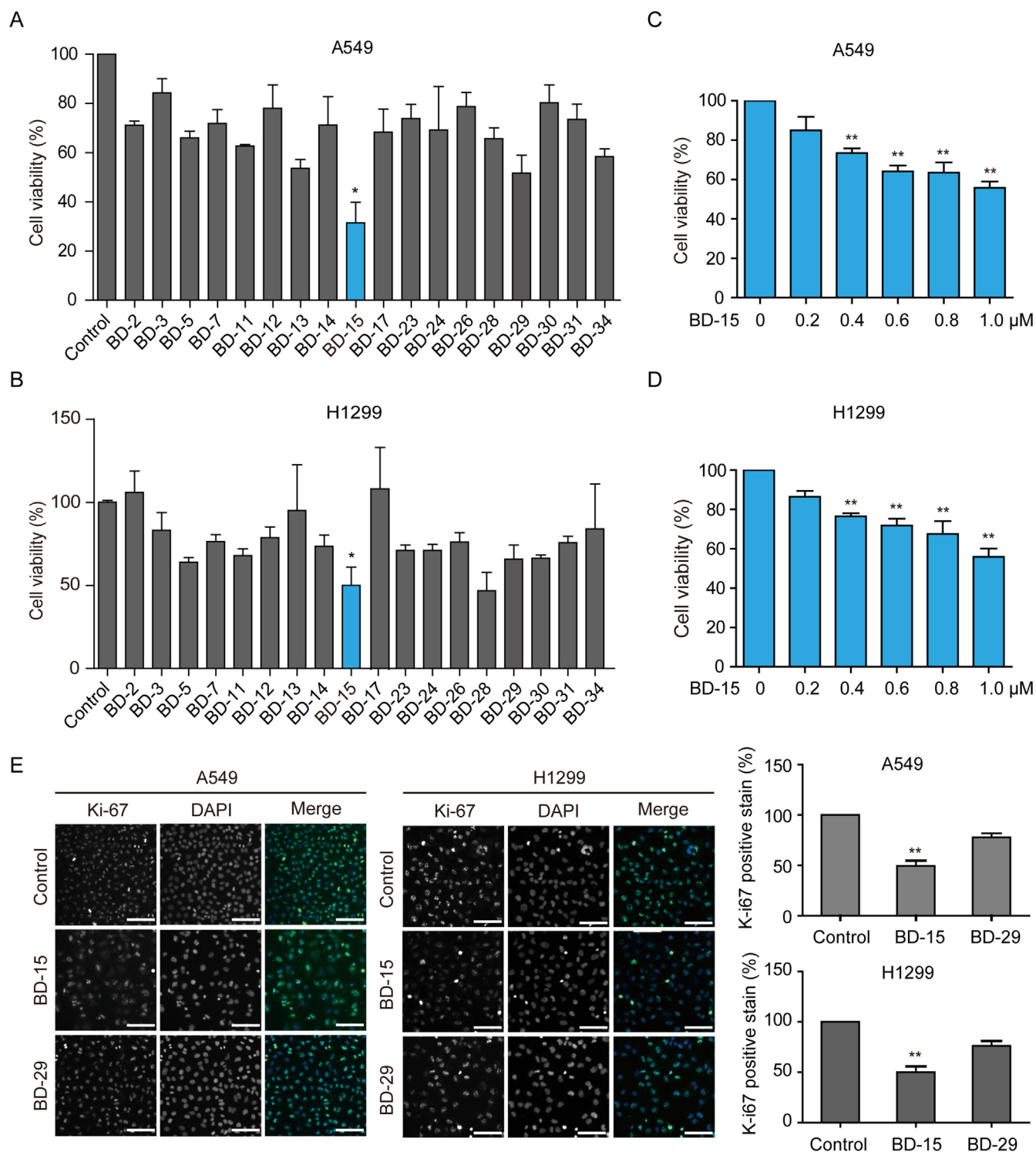


Figure 1. The bisindolylmaleimide derivative BD-15 decreases cell viability and inhibits cell proliferation. A and B A549 and H1299 cells were treated with a series of bisindolylmaleimide derivatives at 1 µM for 24 h, and MTT assays were performed to detect cell viability. C and D Gradient concentration of BD-15 (0.2, 0.4, 0.6, 0.8, 1.0 µM) were used to incubate A549 and H1299 cells for 24 h and cell viability was measured by MTT assays. E Images of Ki-67 staining in A549 and H1299 cells treated with 1 µM BD-15 for 24 h. Scale bar, 100 µm. The ratio of Ki-67 positive cells was quantified. Data are mean ± SEM; n = 3; *p < 0.05; **p < 0.01.

treated group in which mice were injected with BD-15 at 20 mg/kg for 2 weeks. Tumor dimensions were measured by a vernier caliper every two days. Tumor volume was calculated as tumor volume = $(L \times W^2)/2$, L means the longest axis of the tumor and W represents the shortest axis of the tumor.

2.10. Statistical analysis

GraphPad Prism software (version 5.0) was used to conduct statistical analysis. All experiments were performed three times as independent replicates. Data are quantified by one-way ANOVA and presented as

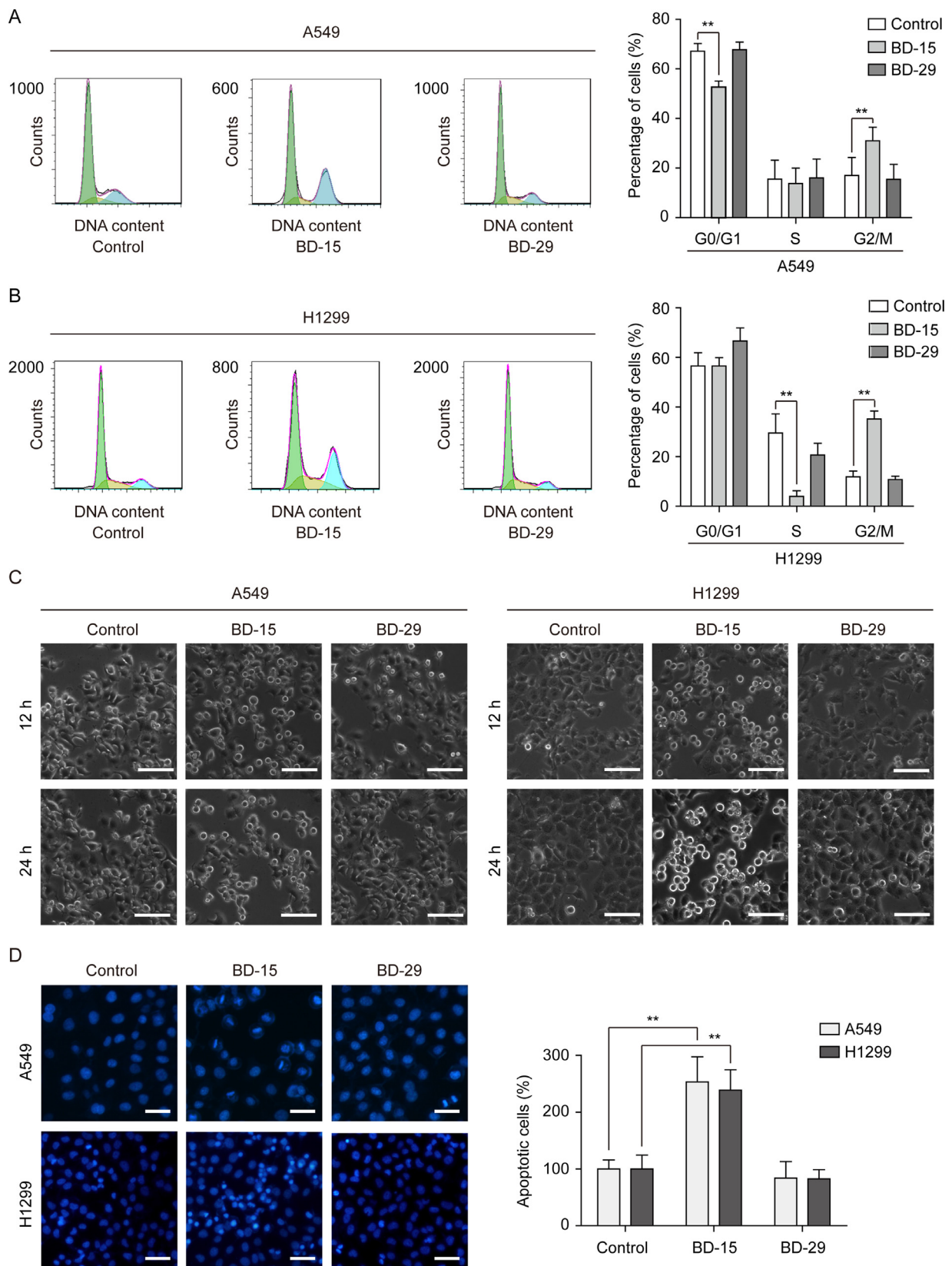


Figure 2. BD-15 induces cell cycle arrest and promotes cellular apoptosis. A and B A549 and H1299 cells were treated with 1 μ M BD-15 and BD-29 for 24 h. Then cell cycle distribution was detected with flow cytometry. The column showed the quantified percentage of A549 and H1299 cells distributed in G0/G1, S and G2/M stages. C Morphologic images of A549 and H1299 cells treated with BD-15 and BD-29 at 1 μ M for 12 and 24 h. D Hoechst 33342 staining was conducted following BD-15 and BD-29 treatment at 1 μ M for 12 h in A549 and H1299 cells. The percentage of apoptotic cells was quantified by counting cells from 3 random view. Data are mean \pm SEM; n = 3; **p < 0.01.

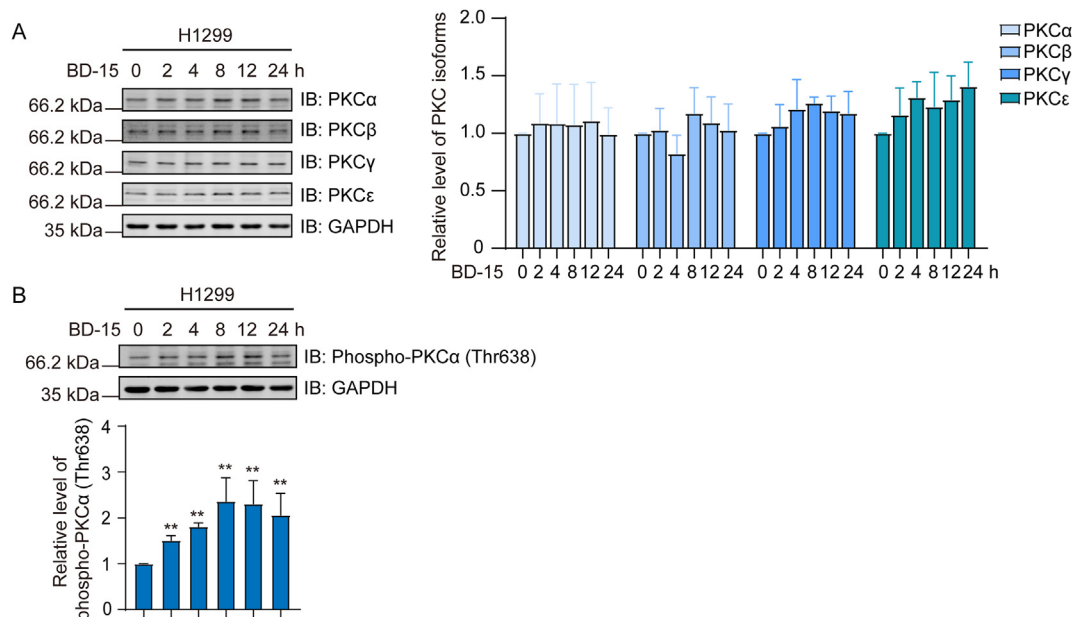


Figure 3. The effect of BD-15 on PKC expression and phosphorylation. A Western blotting analysis of the expression of PKC α , β , γ , and ϵ in H1299 cells treated with BD-15 at 1 μ M for 2, 4, 8, 12 and 24 h. The relative levels of these PKC isoforms were quantified. B Western blotting analysis of the phosphorylated levels of PKC α in H1299 cells treated with BD-15 at 1 μ M for 2, 4, 8, 12 and 24 h. The column charts represent the quantified levels of phospho-PKC α . Data are mean \pm SEM; n = 3; **p < 0.01.

mean \pm SEM. P value less than 0.05 were considered as significant difference.

3. Results

3.1. The bisindolylmaleimide derivative BD-15 inhibits A549 and H1299 cell growth

To investigate potential chemicals regulating PKC signaling, we generated a series of bisindolylmaleimide derivatives. Utilizing this small molecule panel, we assessed their inhibitory effects on NSCLC cells A549 and H1299 by performing MTT assays. As a result, BD-15 showed the strongest inhibition on both A549 and H1299 cell growth (Figure 1A, B, and Supplementary Fig. 1). Moreover, BD-15 dose-dependently decreased cell viability in A549 and H1299 cell lines with the concentrations of 0.2, 0.4, 0.6, 0.8 and 1 μ M (Figure 1C, D). The nuclear protein Ki-67 is a well-established proliferation marker. Immunofluorescence analysis with anti-Ki-67 antibody showed that the percentage of Ki-67-positive cells was dramatically reduced in A549 and H1299 cells treated with BD-15, but no significant changes were recorded in control group treated with BD-29 (bisindolylmaleimide) (Figure 1E). Results from both MTT and immunofluorescence assays confirmed the tumor-suppressive effects of BD-15 against NSCLC cells *in vitro*.

3.2. BD-15 induces cell cycle arrest and promotes cellular apoptosis

We next examined the influence of BD-15 on cell cycle and apoptosis, which are two processes closely involved in tumor initiation and development. Flow cytometry assays were conducted to investigate cell cycle distribution in cells treated with BD-15. Results showed that BD-15 significantly augmented the percentages of cells in G2/M phase in both A549 and H1299 cells, while BD-29 had little effects on cell cycle transition (Figure 2A, B). Morphological observation showed that A549 and H1299 cells became round and detached from the bottom of the dish with BD-15 treatment, while cells treated with BD-29 showed no obvious change compared to the control group (Figure 2C). Hoechst 33342 staining revealed that the apoptosis ratios in A549 and H1299 cells were dramatically increased with BD-15 treatment, and there was no

significant difference in BD-29-treated cells compared to the control group (Figure 2D). These results demonstrated that BD-15 arrested cell cycle progression and promoted apoptosis, thus providing explanations for its inhibitory effects on cell growth.

3.3. BD-15 confers enhanced phosphorylation of PKC substrates

Given that several bisindolylmaleimide derivatives were known to interfere with PKC signaling, we wondered whether BD-15 also suppressed cancer cell growth through regulating PKC signal output. Therefore, we first evaluated the effect of BD-15 on the expression of PKC α , β , γ and ϵ , for their close correlation with NSCLC development. Western blotting results showed these PKC levels were not affected by BD-15 (Figure 3A and Supplementary Fig. 3A). Nevertheless, the phosphorylated levels of PKC α were significantly elevated with BD-15 treatment (Figure 3B and Supplementary Fig. 3B).

Next, we performed Western blotting assays to detect the phosphorylation of PKC substrates with BD-15 treatment for 2, 4, 8, 12, and 24 h in A549 and H1299 cells. It is interesting to observe that BD-15 dramatically enhanced the phosphorylated levels of PKC substrates in a time-dependent manner (Figure 4A, B, and Supplementary Fig. 4A, B). However, the phosphorylation of PKC substrates showed little response to BD-29 (Figure 4A, B, and Supplementary Fig. 4A, B). ERK1/2 are known as representative downstream targets of PKC signaling [18]. Consistently, ERK1/2 phosphorylation was significantly increased with BD-15 treatment but appeared unchanged with BD-29 incubation (Figure 4C, D, and Supplementary Fig. 4C, D). Therefore, our results suggest that BD-15 treatment leads to effective upregulation of PKC signaling. In addition, we analyzed the expression of nine PKC isozymes in lung adenocarcinoma (LUAD) and lung squamous cell carcinoma (LUSC) using TCGA dataset, and found PKC isozyme levels (besides PKC ζ) were generally decreased in both tumors compared with those in normal tissues, among which PKC β , ϵ , η and ζ exhibited significant downregulation in cancerous tissues (Figure 5). For the high mutation rate of PKC in NSCLC, we searched the catalogue of somatic mutations in cancer (COSMIC) for the mutations of PKC in collected A549 and H1299 cell lines. PKC β and PKC ζ shows mutations in A549 and H1299 cells respectively, with substitutions, deletions, copy number variants and aberrant gene expression

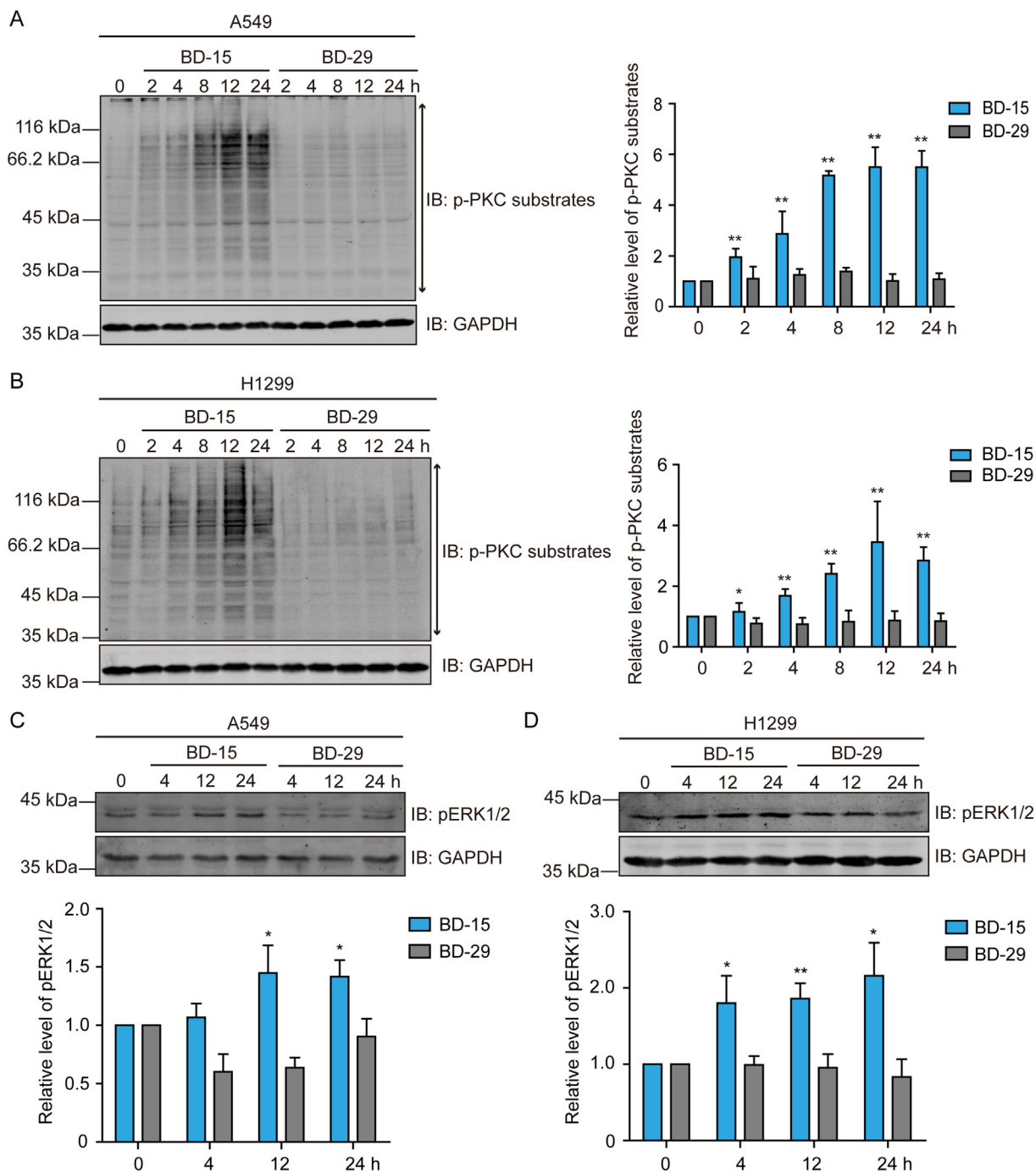


Figure 4. BD-15 enhances the phosphorylation of PKC substrates. A and B Western blotting analysis of the phosphorylation of PKC substrate in A549 (A) and H1299 (B) cells treated with BD-15 and BD-29 at 1 μ M for 2, 4, 8, 12 and 24 h. The relative level of phosphorylated PKC substrates (p-PKC substrates) were quantified. C and D Western blotting analysis of phosphorylated levels of ERK1/2 in A549 (C) and H1299 (D) cells treated with BD-15 and BD-29 at 1 μ M for 4, 12 and 24 h. The column charts represent the quantified level of pERK1/2. Data are mean \pm SEM; n = 3; * p < 0.05; ** p < 0.01.

(Supplementary Fig. 2). Collectively, these results support the notion that PKC proteins demonstrate tumor-suppressive effects in lung adenocarcinoma, and BD-15-induced PKC signal amplification effectively inhibits cancer cell proliferation.

3.4. BD-15 promotes p21 expression and elevates p21 phosphorylation

p21 is a well-known cell cycle inhibitor. It has been reported that PKC α can induce pERK-activated SP1 binding to the promoter region of the p21-encoding *CDKN1A*, thus elevating p21 expression and leading to cell cycle arrest [18]. We next investigated whether PKC signal amplification by

BD-15 treatment led to cell cycle blockage through p21 upregulation. Indeed, Western blotting results showed that p21 expression was elevated by BD-15 treatment after 12 and 24 h, with no effect observed when cells were treated with BD-29 (Figure 6A, and Supplementary Fig. 5A). As a result, our data suggest that BD-15-induced PKC signal amplification promotes p21 expression and contributes to cell cycle arrest.

On the other hand, p21 can also protect cells from apoptosis, which is seemingly contradictory to our observation that BD-15 induces apoptosis in A549 and H1299 cells. Although it has been reported that p21 binds to pro-caspase-3 and leads to caspase-3 inactivation [19, 20], p21 phosphorylation was demonstrated to block the association between p21 and

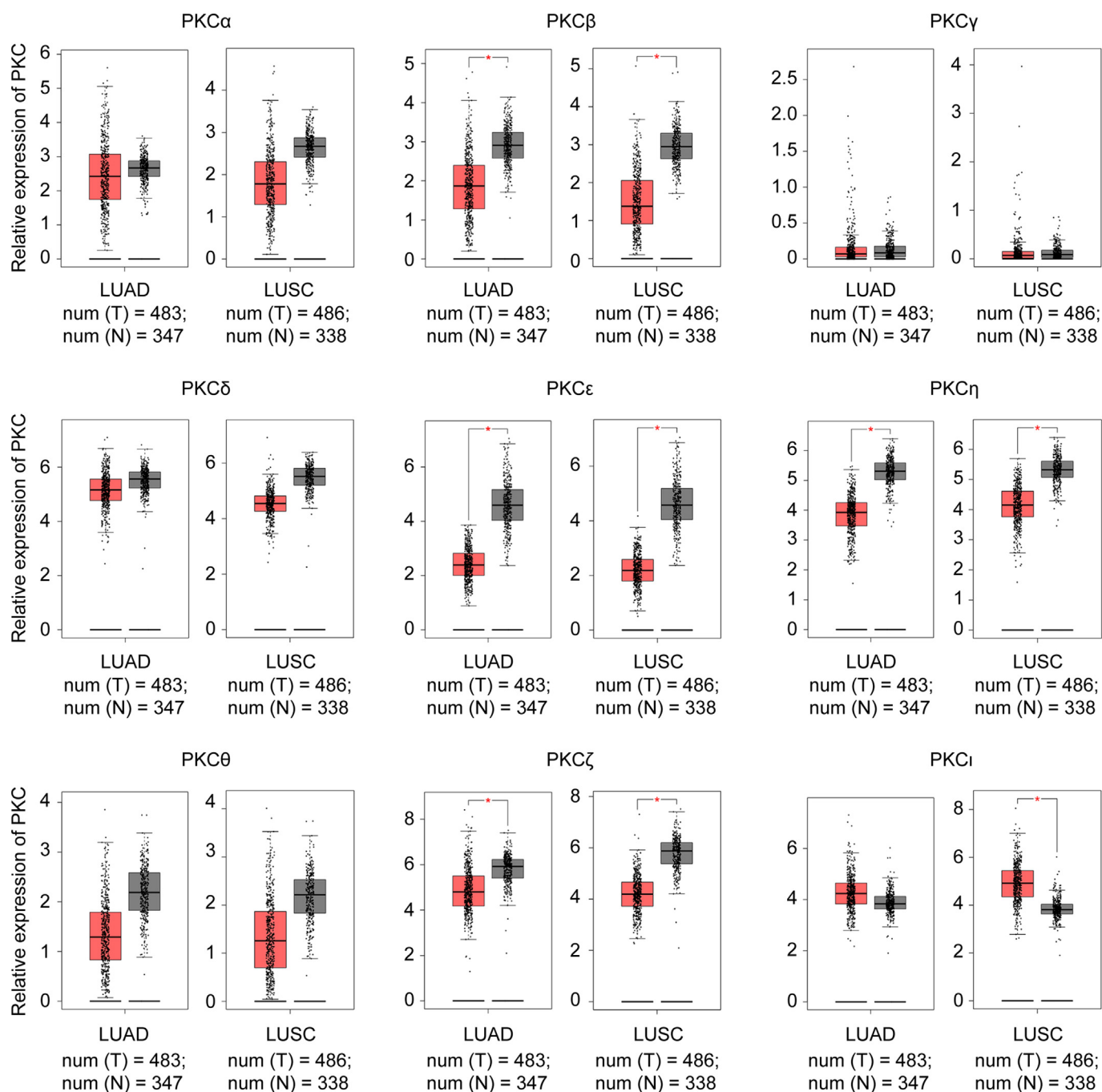


Figure 5. Bioinformatic analysis of the expression levels of PKC in LUAD, LUSC and normal tissues. GEPIA (Gene Expression Profiling Interactive Analysis) was used to analyze the levels of the nine PKC isozyms (PKC α , β , γ , δ , ϵ , η , θ , ζ and ι) in tumor (T) and normal tissues (N), with * indicates p-value cutoff 0.01.

its interacting proteins [21]. Based on these evidence, we speculate that BD-15 might also induce p21 phosphorylation and thus block the binding of p21 to pro-caspase-3, leading to caspase-3 activation and cellular apoptosis. To explore this potential, we examined p21 phosphorylation in A549 and H1299 cells treated with BD-15 with or without lambda phosphatase to confirm phosphorylation. BD-15 treatment led to the detection of an extra higher molecular weight species using anti-p21 antibody, which was effectively dissolved by the incubation with lambda phosphatase (Figure 6B, and Supplementary Fig. 5B). These results infer that BD-15 treatment promotes p21 phosphorylation. As caspase-3 cleavage is a vital step of caspase-3 activation, we next performed Western blotting assays to detect cleaved caspase-3 with or without BD-15 treatment. The results showed that the levels of cleaved caspase-3 were increased with

BD-15 treatment after 12 and 24 h, but no effect was detected in BD-29-treated groups (Figure 6C, D, and Supplementary Fig. 5C). Accompanied by caspase-3 cleavage, the levels of Bcl-2 were also decreased by BD-15 (Figure 6C, D, and Supplementary Fig. 5C). Hence, these findings suggest that BD-15 induces cell cycle arrest via augmenting p21 expression and promotes apoptosis through increasing p21 phosphorylation.

3.5. BD-15 suppresses tumor xenograft growth in nude mouse models

Next, we evaluated the anti-cancer efficiency of BD-15 *in vivo* by monitoring the growth of tumor xenografts in nude mice. A549 and H1299 cells were subcutaneously injected into nude mice and tumor

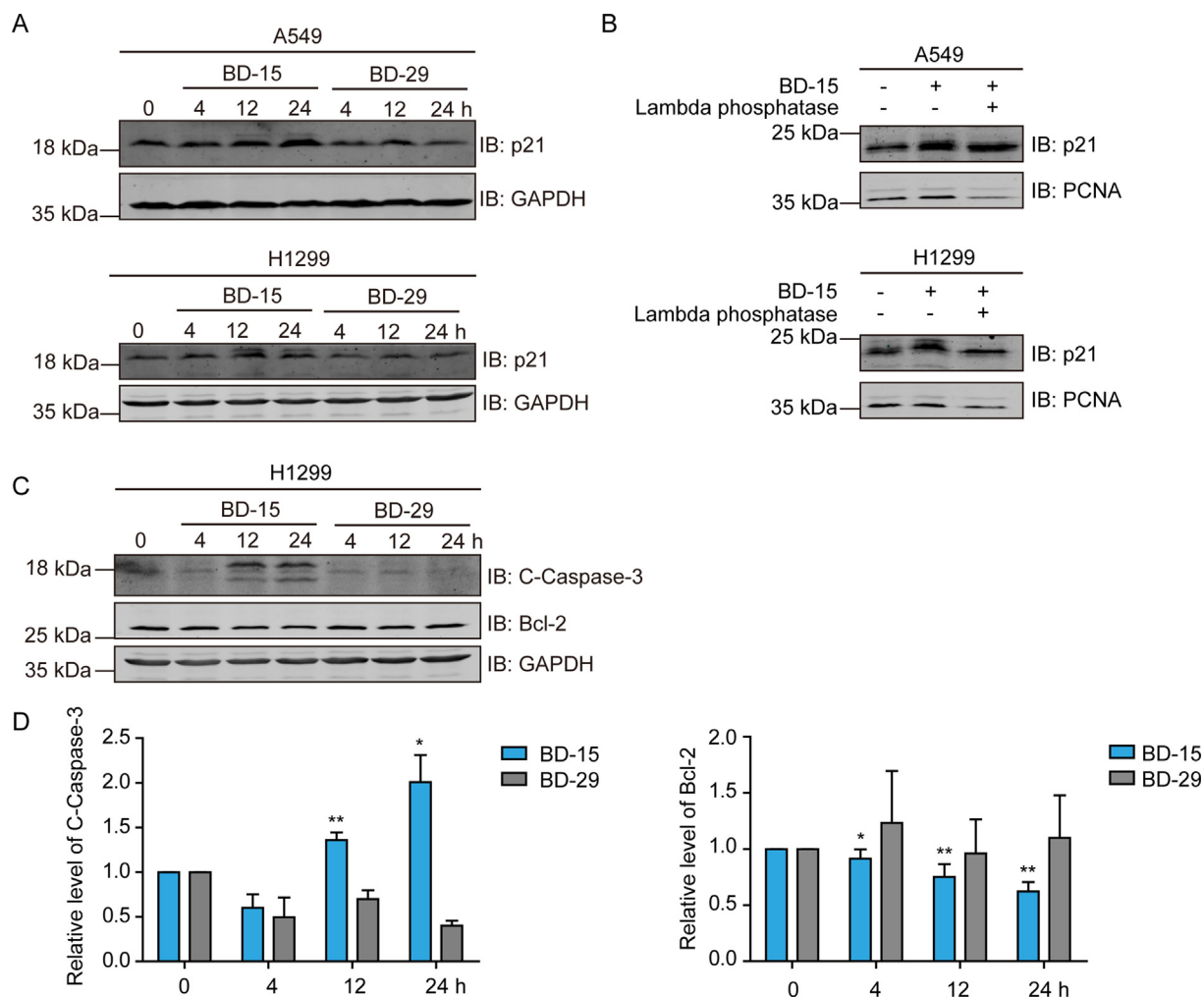


Figure 6. BD-15 promotes p21 expression and elevates p21 phosphorylation. **A** p21 expression was detected by Western blotting in A549 and H1299 cells treated with BD-15 and BD-29 at 1 μ M for 4, 12 and 24 h. **B** Western blotting analysis of p21 phosphorylation in A549 and H1299 cells treated with 1 μ M BD-15 for 24 h with or without lambda phosphatase. **C** H1299 cells were treated with BD-15 and BD-29 at 1 μ M for indicated times. Western blotting was conducted to examine the level of cleaved-caspase-3 (C-Caspase-3) and Bcl-2. **D** The data from C were quantified as shown in the column chart. Data are mean \pm SEM; n = 3; * p < 0.05, ** p < 0.01.

formation was observed in mice with these subcutaneous NSCLC xenografts. When tumor length reached about 6–7 mm on average, BD-15 (20 mg/kg) was administered intraperitoneally every day for 15 days and vehicle was used as control. Measurements of tumor volumes were performed every other day. Xenograft growth curves showed that tumor growth was significantly deterred in BD-15-treated groups with both A549 and H1299 xenografts (Figure 7A, B). Therefore, these results confirmed the tumor-suppressive effects of BD-15 against NSCLC growth *in vivo*.

4. Discussion

With the tumor-suppressive roles of PKC proteins becoming established [3], future therapeutic strategies on cancer treatment through targeting PKC would be focused on restoring rather than inhibiting PKC activities. Given that loss-of-function PKC mutations are frequently occurring in NSCLC, suggesting this cancer type as a suitable model for PKC interference. In the current study, we identified a small molecule BD-15 that effectively amplified PKC signal output, by which it markedly inhibited NSCLC cell growth. PKC signal amplification incurred by BD-15 promoted p21 expression and increased p21 phosphorylation, leading to cell cycle arrest and apoptosis (Figure 7C).

PKC mutations are detected in about 20–25% of lung cancer, colorectal cancer and melanoma, while are occurring in less than 5% of

ovarian cancer, glioblastoma and breast cancer [5]. Dominant negative PKC mutations in lung cancer are mainly associated with isoforms PKC α , β , γ and η (5). Moreover, NexBio database analysis also revealed that NSCLC expressed decreased levels of PKC α [22]. Bioinformatic analysis using the GEPIA website showed significantly reduced expression of PKC β , ϵ , η and ζ in LUAD. The PKC ligand DAG and its analogues PDBu, PMA, and prostratin were shown to bind and activate PKC signaling. Both direct and indirect activators of PKC signaling in NSCLC were also reported, including small molecules 10-Me-aplog-1 and ingenol 3,20 dibenzoate (IDB). The compound 10-Me-aplog-1 was reported as a PKC activator that inhibited A549 cell proliferation in a PKC α -dependent manner [9]. The natural product IDB is a kind of nPKC activator and delayed NSCLC progression via enhancing the NK cell-mediated lysis of NSCLC cells [23]. Therefore, conventional PKCs (cPKC) and novel PKCs (nPKC) are the most likely isoforms that function in NSCLC development, while the specific PKC isoforms that are influenced by BD-15 await further exploration.

p21 plays a dual role in tumor growth regulation, including both cell cycle arrest and apoptosis suppression. Here, we observed that p21 protein level was increased by BD-15 treatment, resulting in NSCLC cell cycle arrest. Meanwhile, it is interesting that BD-15 triggers apoptosis, which seems to be linked to p21 phosphorylation. Six phosphorylation sites have been identified in p21, including T57, S130, T145, S146, S153 and S160, that are involved in various intracellular processes [24]. Among distinct

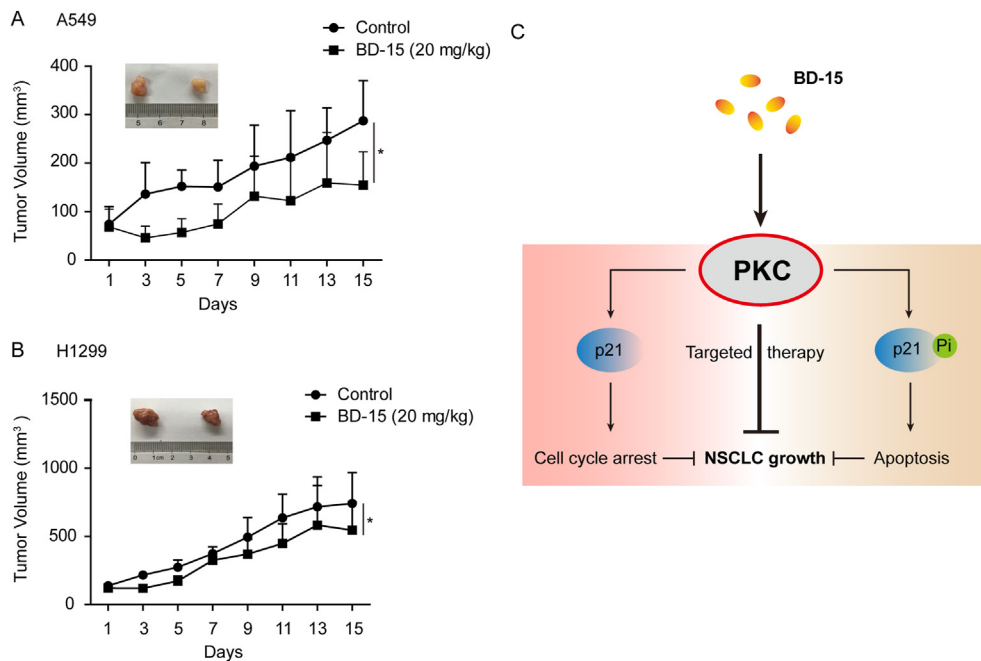


Figure 7. BD-15 suppresses tumor growth in nude mouse models. BALB/c nude mice carrying A549 and H1299 xenografts were divided into 2 groups respectively. Control group received saline and another group was injected with BD-15 (20 mg/kg). Tumor volume was measured every two days. A The growth curve of tumor volume in A549 xenograft-bearing mice. B The growth curve of tumor volume in H1299 xenograft-bearing mice. Data are mean \pm SEM; * $p < 0.05$. C A working model depicting the inhibitory effect of BD-15 on NSCLC cell growth. BD-15 enhances PKC signal output, and PKC signal amplification promotes p21 expression and increases p21 phosphorylation, leading to cell cycle arrest and apoptosis.

kinases phosphorylating p21, PKC is responsible for the phosphorylation on the S146 and S160 sites, and thus blocks the binding of p21 to PCNA [25]. In addition, it has been reported that p21 binds to pro-caspase-3 within 15–33 amino acid region and thus inhibits caspase-3 activation. Besides, PKC ζ shows positive correlation with caspase-3 activity in human intestinal tumor [26]. Our findings indicate that p21 phosphorylation is likely a key factor in BD-15-induced apoptosis. PKC activation increases p21 phosphorylation, and thus blocks the interaction between p21 and pro-caspase-3 to promote caspase-3 cleavage, leading to enhanced apoptosis. The essential role of p21 phosphorylation mediated by PKC provides an explanation to the apoptosis induction stimulated by BD-15.

In summary, our present study identified a bisindolylmaleimide derivative named BD-15 as an effective compound to amplify PKC signaling, which showed strong anti-cancer effects to inhibit NSCLC growth both *in vitro* and *in vivo*. Mechanistically, BD-15 promoted p21 expression to arrest cell cycle progression, as well as increased p21 phosphorylation to induce apoptosis through promoting caspase3 cleavage. Our findings provide a paradigm of targeted therapeutic strategy against NSCLC through inducing PKC signal amplification and warrant further investigation.

Declarations

Author contribution statement

Shuyan Liu; Yayun Zhang; Qianyi Yang: Performed the experiments; Analyzed and interpreted the data.

Yingqiu Zhang; Han Liu: Analyzed and interpreted the data; Contributed reagents, materials, analysis tools or data.

Mu-Hua Huang; Ruoyu Wang: Conceived and designed the experiments.

Faqiang Lu: Conceived and designed the experiments; Wrote the paper.

Funding statement

Shuyan Liu was supported by China Postdoctoral Science Foundation [2020M680921], National Natural Science Foundation of China [82103146].

Data availability statement

Data included in article/supp. material/referenced in article.

Declaration of interest's statement

The authors declare no conflict of interest.

Additional information

Supplementary content related to this article has been published online at <https://doi.org/10.1016/j.heliyon.2022.e10657>.

References

- [1] N. Isakov, Protein kinase C (PKC) isoforms in cancer, tumor promotion and tumor suppression, *Semin. Cancer Biol.* 48 (2018) 36–52.
- [2] A.C. Newton, J. Brognard, Reversing the paradigm: protein kinase C as a tumor suppressor, *Trends Pharmacol. Sci.* 38 (5) (2017) 438–447.
- [3] A.C. Newton, Protein kinase C as a tumor suppressor, *Semin. Cancer Biol.* 48 (2018) 18–26.
- [4] T. Kawano, J. Inokuchi, M. Eto, M. Murata, J.H. Kang, Activators and inhibitors of protein kinase C (PKC): their applications in clinical trials, *Pharmaceutics* 13 (11) (2021).
- [5] C.E. Antal, A.M. Hudson, E. Kang, C. Zanca, C. Wirth, N.L. Stephenson, et al., Cancer-associated protein kinase C mutations reveal kinase's role as tumor suppressor, *Cell* 160 (3) (2015) 489–502.
- [6] L.L. Zhang, F.F. Cao, Y. Wang, F.L. Meng, Y. Zhang, D.S. Zhong, et al., The protein kinase C (PKC) inhibitors combined with chemotherapy in the treatment of advanced non-small cell lung cancer: meta-analysis of randomized controlled trials, *Clin. Transl. Oncol.* : official publication of the Federation of Spanish Oncology Societies and of the National Cancer Institute of Mexico 17 (5) (2015) 371–377.
- [7] M.A. Lum, C.J. Barger, A.H. Hsu, O.V. Leontieva, A.R. Black, J.D. Black, Protein kinase alpha (PKC α) is resistant to long term desensitization/down-regulation by prolonged diacylglycerol stimulation, *J. Biol. Chem.* 291 (12) (2016) 6331–6346.
- [8] C. Bessa, J. Soares, L. Raimundo, J.B. Loureiro, C. Gomes, F. Reis, et al., Discovery of a small-molecule protein kinase C δ -selective activator with promising application in colon cancer therapy, *Cell Death Dis.* 9 (2) (2018) 23.
- [9] Y. Hanaki, Y. Shikata, M. Kikumori, N. Hotta, M. Imoto, K. Irie, Identification of protein kinase C isozymes involved in the anti-proliferative and pro-apoptotic activities of 10-Methyl-aplog-1, a simplified analog of debromoaplysiatoxin, in several cancer cell lines, *Biochem. Biophys. Res. Commun.* 495 (1) (2018) 438–445.
- [10] K. Evangelou, P. Galanos, V.G. Gorgoulis, The Janus face of p21, *Molecular & cellular oncology* 3 (5) (2016), e1215776.
- [11] A. Karimian, Y. Ahmadi, B. Yousefi, Multiple functions of p21 in cell cycle, apoptosis and transcriptional regulation after DNA damage, *DNA Repair* 42 (2016) 63–71.

- [12] J. Chen, G.Q. Li, L. Zhang, M. Tang, X. Cao, G.L. Xu, et al., Complement C5a/C5aR pathway potentiates the pathogenesis of gastric cancer by down-regulating p21 expression, *Cancer Lett.* 412 (2018) 30–36.
- [13] H. Nam, M.M. Kim, Ursolic acid induces apoptosis of SW480 cells via p53 activation, *Food Chem. Toxicol.* : an international journal published for the British Industrial Biological Research Association 62 (2013) 579–583.
- [14] L. Liu, G. Chen, B. Wang, L. Chen, S. Wang, Z. Liu, et al., Effect of Fanbaicao (herba potentillae discoloris) oil on the expression of p21 and CDK4 in HepG2 cells, *Journal of traditional Chinese medicine = Chung i tsa chih ying wen pan* 36 (4) (2016) 496–503.
- [15] M.H. Huang, Y.C. Gao, F.L. Yang, Y.J. Luo, 3,4-Bis[1-(prop-2-yn-yl)-1H-indol-3-yl]-1H-pyrrole-2,5-dione, *Acta Crystallogr., Sect. E: Struct. Rep. Online* 69 (Pt 6) (2013) o924–o925.
- [16] J. Zhang, S. Liu, Q. Li, Y. Shi, Y. Wu, F. Liu, et al., The deubiquitylase USP2 maintains ErbB2 abundance via counteracting endocytic degradation and represents a therapeutic target in ErbB2-positive breast cancer, *Cell Death Differ.* 27 (9) (2020) 2710–2725.
- [17] S. Liu, T. Wang, Y. Shi, L. Bai, S. Wang, D. Guo, et al., USP42 drives nuclear speckle mRNA splicing via directing dynamic phase separation to promote tumorigenesis, *Cell Death Differ.* 28 (8) (2021) 2482–2498.
- [18] Y.Y. Lee, M.S. Ryu, H.S. Kim, M. Suganuma, K.Y. Song, I.K. Lim, Regulations of reversal of senescence by PKC isozymes in response to 12-O-Tetradecanoylphorbol-13-Acetate via nuclear translocation of pErk1/2, *Mol. Cell.* 39 (3) (2016) 266–279.
- [19] A. Suzuki, Y. Tsutomi, K. Akahane, T. Araki, M. Miura, Resistance to Fas-mediated apoptosis: activation of caspase 3 is regulated by cell cycle regulator p21WAF1 and IAP gene family ILP, *Oncogene* 17 (8) (1998) 931–939.
- [20] A. Suzuki, Y. Tsutomi, M. Miura, K. Akahane, Caspase 3 inactivation to suppress Fas-mediated apoptosis: identification of binding domain with p21 and ILP and inactivation machinery by p21, *Oncogene* 18 (5) (1999) 1239–1244.
- [21] M.T. Scott, N. Morrice, K.L. Ball, Reversible phosphorylation at the C-terminal regulatory domain of p21(Waf1/Cip1) modulates proliferating cell nuclear antigen binding, *J. Biol. Chem.* 275 (15) (2000) 11529–11537.
- [22] K.S. Hill, E. Erdogan, A. Khor, M.P. Walsh, M. Leitges, N.R. Murray, et al., Protein kinase Calpha suppresses Kras-mediated lung tumor formation through activation of a p38 MAPK-TGFbeta signaling axis, *Oncogene* 33 (16) (2014) 2134–2144.
- [23] C. Gong, C. Yao, Z. Xu, Z. Ni, X. Zhu, L. Wang, et al., Enhancement of NK cell-mediated lysis of non-small lung cancer cells by nPKC activator, ingenol 3,20 dibenzoate, *Mol. Immunol.* 83 (2017) 23–32.
- [24] E.S. Child, D.J. Mann, The intricacies of p21 phosphorylation: protein/protein interactions, subcellular localization and stability, *Cell Cycle* 5 (12) (2006) 1313–1319.
- [25] M.T. Scott, A. Ingram, K.L. Ball, PDK1-dependent activation of atypical PKC leads to degradation of the p21 tumour modifier protein, *EMBO J.* 21 (24) (2002) 6771–6780.
- [26] L. Ma, Y. Tao, A. Duran, V. Llado, A. Galvez, J.F. Barger, et al., Control of nutrient stress-induced metabolic reprogramming by PKCzeta in tumorigenesis, *Cell* 152 (3) (2013) 599–611.